Erratum: "Air/Water Counter-Current Flow Experiments in a Model of the Hot Leg of a Pressurized Water Reactor" [Journal of Engineering for Gas Turbines and Power, 2009, 131(2), p. 022905]

Christophe Vallée, Deendarlianto, Matthias Beyer, Dirk Lucas and Helmar Carl

An error in the implementation into the test facility of the air flow meter used during the experiments was noticed after publication of the paper. As a consequence, the raw flow rates recorded by the digital data acquisition system with this flow meter are wrong. In order to correct the measured flow rates, a calibration curve was recorded with a certified rotameter. The obtained calibration points could be correlated in order to obtain the correction function applied to the raw measuring values. This resulted in the following modifications compared to the original paper:

- p. 1, last two sentences of the Abstract: A good overall agreement was obtained, especially for the zero liquid penetration, while the slope of the CCFL characteristics was lower compared to previous work. This deviation may be attributed to the rectangular cross-section of the hot leg model.
- p. 3, end of Sec. 3.1: (…) the air mass flow rate was varied between 0.23 and 0.41 kg/s.
- p. 3, Sec. 3.2.1, point (2), line 1: At an injected air mass flow rate of 0.38 kg/s (…).
- p. 3, Sec. 3.2.1, point (2), antepenultimate line: ($\dot{m}_G = 0.395$ kg/s)
- p. 3, Sec. 3.2.1, point (3): With a further increase of the air mass flow rate up to 0.41 kg/s (…).
- p. 4, caption of Fig. 4: Flow behavior during the countercurrent flow of air and water at a water flow rate of 0.3 kg/s, and a pressure of 3.0 bar. (*a*) $\dot{m}_G = 0.345$ kg/s, t = 21.00 s; (*b*) $\dot{m}_G = 0.395$ kg/s, t = 76.59 s; and (*c*) $\dot{m}_G = 0.41$ kg/s, t = 97.92 s.
- p. 4, Sec. 3.2.2, point (2), line 1: At an injected air mass flow rate of 0.38 kg/s (…).
- pp. 4 and 5, Sec. 3.2.2, point (3), lines 1 and 2: The zero liquid penetration is reached with a further increase of the air mass flow rate up to 0.41 kg/s (…).
- p. 5, caption of Fig. 6. Flow behavior observed during the countercurrent flow experiment at a water flow rate of 0.9 kg/s and pressure of 3.0 bar. (*a*) Before the onset of flooding (t = 63.00 s, $\dot{m}_G = 0.345$ kg/s); (*b*) at the onset of flooding (t = 78.00 s, $\dot{m}_G = 0.38$ kg/s); (*c*) t = 78.60 s, $\dot{m}_G = 0.38$ kg/s; (*d*) t = 79.10 s, $\dot{m}_G = 0.38$ kg/s; (*e*) t = 96.00 s, $\dot{m}_G = 0.41$ kg/s; (*f*) t = 108.90 s, $\dot{m}_G = 0.41$ kg/s.
- p. 7, Sec. 4.3, 3rd sentence, lines 5-8: As shown in the flooding diagram (Fig. 8), the present data comes closer to the correlations reported by Ohnuki et al., Navarro, Lopez-De-Bertodano, Kang et al., and Kim and No, especially close to the zero liquid penetration.
- p. 7, Sec. 4.3, 1st paragraph: delete the last sentence.
- p. 7, Sec. 5, 2nd paragraph, 3rd sentence, lines 5-7: The obtained flooding curve is similar to those reported by other investigators: the zero liquid penetration agrees especially well, but the slope of the characteristics is lower.

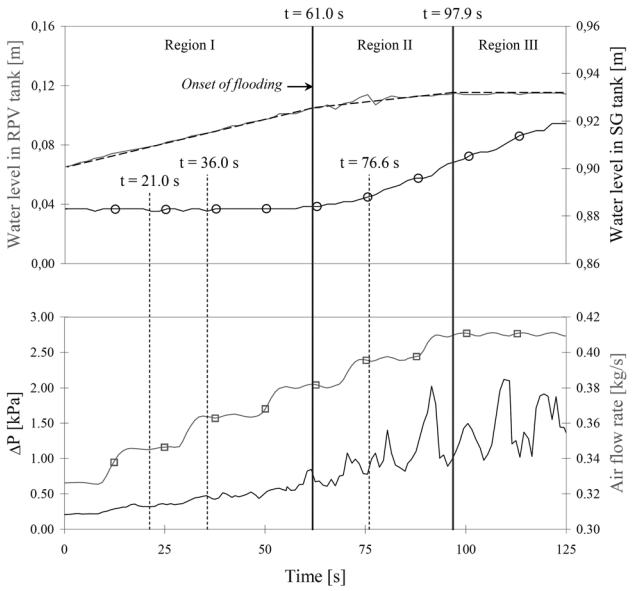

Fig. 3 Variation of the water levels in the RPV simulator (top diagram, top gray curve) and in the SG separator (top diagram, bottom black curve with points), of the air mass flow rate (bottom diagram, top gray curve with squares) and of the pressure drop over the test-section (bottom diagram, bottom black curve), measured at a water mass flow rate of 0.3 kg/s and a pressure of 3.0 bar

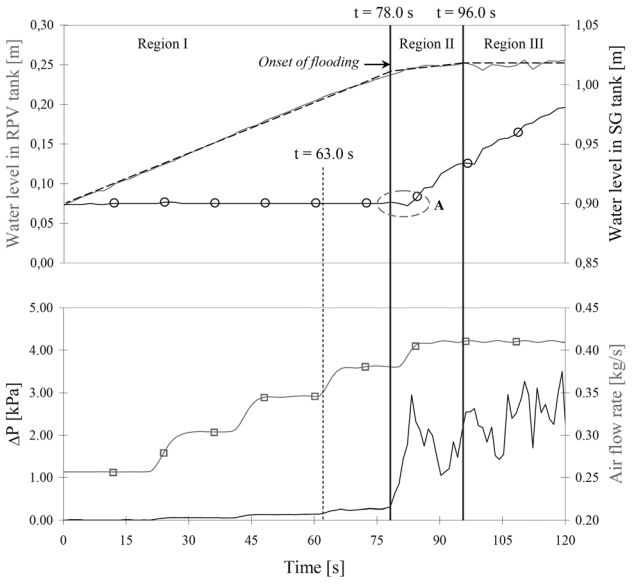

Fig. 5 Variation of the water levels in the SG separator (top diagram, bottom black curve with points) and in the RPV simulator (top diagram, top gray curve), of the pressure difference between the vessels (bottom diagram, bottom black curve) and of the air mass flow rate (bottom diagram, top gray curve with squares), measured at a water mass flow rate of 0.9 kg/s and a pressure of 3.0 bar

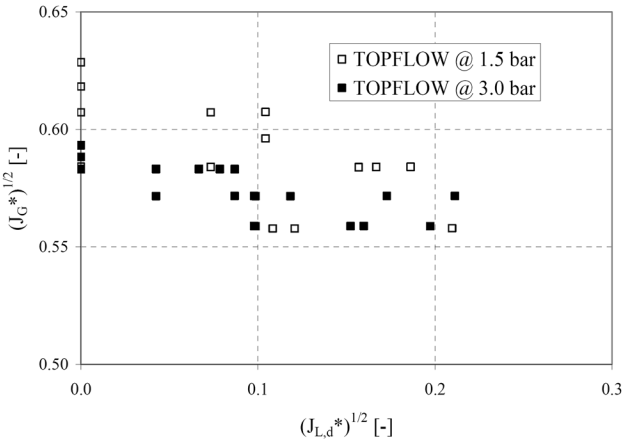

Fig. 7 Flooding diagram obtained for the hot leg model

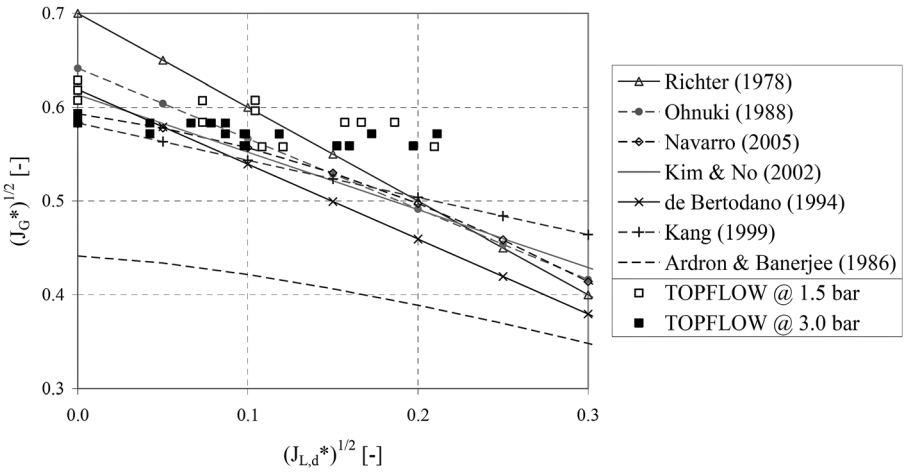

Fig. 8 Comparison of the present data with different CCFL correlations obtained for hot leg typical geometries